




Article

Multiobjective Optimization of Fuzzy System for Cardiovascular Risk Classification

Hanna C. Villamil ^{*}, Helbert E. Espitia  and Lilian A. Bejarano 

Facultad de Ingeniería, Universidad Distrital Francisco José de Caldas, Bogotá 110231, Colombia; heespitiac@udistrital.edu.co (H.E.E.); lbejarano@udistrital.edu.co (L.A.B.)

* Correspondence: hcvillamilo@udistrital.edu.co

Abstract: Since cardiovascular diseases (CVDs) pose a critical global concern, identifying associated risk factors remains a pivotal research focus. This study aims to propose and optimize a fuzzy system for cardiovascular risk (CVR) classification using a multiobjective approach, addressing computational aspects such as the configuration of the fuzzy system, the optimization process, the selection of a suitable solution from the optimal Pareto front, and the interpretability of the fuzzy logic system after the optimization process. The proposed system utilizes data, including age, weight, height, gender, and systolic blood pressure to determine cardiovascular risk. The fuzzy model is based on preliminary information from the literature; therefore, to adjust the fuzzy logic system using a multiobjective approach, the body mass index (BMI) is considered as an additional output as data are available for this index, and body mass index is acknowledged as a proxy for cardiovascular risk given the propensity for these diseases attributed to surplus adipose tissue, which can elevate blood pressure, cholesterol, and triglyceride levels, leading to arterial and cardiac damage. By employing a multiobjective approach, the study aims to obtain a balance between the two outputs corresponding to cardiovascular risk classification and body mass index. For the multiobjective optimization, a set of experiments is proposed that render an optimal Pareto front, as a result, to later determine the appropriate solution. The results show an adequate optimization of the fuzzy logic system, allowing the interpretability of the fuzzy sets after carrying out the optimization process. In this way, this paper contributes to the advancement of the use of computational techniques in the medical domain.

Keywords: body mass index; cardiovascular diseases; healthcare; multiobjective optimization; fuzzy system; overweight; Pareto front



Citation: Villamil, H.C.; Espitia, H.E.; Bejarano, L.A. Multiobjective Optimization of Fuzzy System for Cardiovascular Risk Classification. *Computation* **2023**, *11*, 147. <https://doi.org/10.3390/computation11070147>

Academic Editor: Simone Brogi

Received: 14 June 2023

Revised: 19 July 2023

Accepted: 21 July 2023

Published: 23 July 2023



Copyright: © 2023 by the authors. Licensee MDPI, Basel, Switzerland. This article is an open access article distributed under the terms and conditions of the Creative Commons Attribution (CC BY) license (<https://creativecommons.org/licenses/by/4.0/>).

1. Introduction

As reported by the world health organization (WHO), cardiovascular disease remains a prominent cause of mortality on a global scale, accounting for approximately 17.9 million deaths on an annual basis. The etiology of heart disease involves various associated risk factors, such as metabolic disorders, obesity, and hypertension, which are believed to exert a potential influence on the progression and development of the condition.

Regarding medical studies, a risk classification of scenarios of cardiovascular disease and metabolic syndrome disease is shown in [1] in cases of obesity with low prevalence. The researchers used data on Japanese patients from 40 to 74 years of age with no cardiovascular disease backgrounds from 10 prospective studies in Japan. The authors state that the metabolic syndrome corresponds to the presence of elevated obesity in the abdominal area, including overweight and other factors like arterial hypertension, high-density lipoprotein cholesterol, or elevated levels of triglycerides. The study shows that similar levels of cardiovascular disease and associated risks in individuals with components of metabolic syndrome with or without issues of obesity or overweight require a mandatory change in lifestyle in both groups.

Additionally, a study related to the estimation of transgender and gender-diverse patients' cardiovascular disease is shown in [2]. According to the authors, transgender people

experience noticeably high mortality rates due to cardiovascular issues; consequently, researchers aim to unveil the impact of statin therapy recommendations regarding gender in the equation of risk estimator. The data used for the equation of disease risk were collected from October 2020 to June 2022, and the 102 patients averaged 43 years of age, and 79% of them were taking gender-affirming hormones. From the observations, the researchers noticed that the scores related to the risk equation predominantly varied depending on the approach in terms of gender and hormone use, which must be considered in studies of cardiovascular health.

The relationship between heightened body mass index and an increased propensity for cardiovascular disease is attributed to surplus adipose tissue; in particular, abdominal adiposity can elevate blood pressure, cholesterol, and triglyceride levels, leading to arterial and cardiac damage [1]. This highlights the importance of having a model to determine the level of risk of cardiovascular disease and the different associated risk factors. Several recent studies have shed light on this relationship. For instance, the study presented in [3] found that body mass index is strongly associated with hypertension. Another study [4] compared the performance of body fat percentage, fat mass index, and body mass index in detecting cardiometabolic outcomes in Brazilian adults. Additionally, the review article [5] discusses the past, present, and future of metabolic syndrome, which is a cluster of risk factors that increase the risk of cardiovascular disease. It is also noteworthy to highlight studies such as [6–8], where it is stated that BMI is not the best measure of health; therefore, this index may be controversial for some healthcare providers.

In order to mitigate the aforementioned risk factors and enhance the effective handling of heart disease, scholars resorted to artificial intelligence (AI) techniques to craft prognostic models and decision-support systems.

This discourse concerns a distinctive optimization technique, commonly known as the multiobjective optimization approach, which entails the harmonization of several objectives. This approach seeks to optimize multiple objectives concurrently by considering the interdependencies between them and the associated trade-offs. The Pareto front is a prevalent mechanism in the field of healthcare, particularly in the context of cardiovascular disease, which serves as a means of visualizing the trade-offs involved in decision-making and pinpointing the most desirable solutions [9–11]. As an illustration, a metaheuristic multiobjective optimization approach is utilized in a study to identify Alzheimer's disease through the use of multimodal data [9]. The Pareto front was employed to enhance the sensitivity and specificity of the detection methodology.

For the context of drinking water systems, a sustainable decision support system was developed using a multiobjective optimization method to improve resistance to cyanide contamination [12].

In addition, the use of AI and optimization methods have been used in transportation [13,14] and environmental management [15]. In one study, a genetic algorithm was used to determine the optimal location for traffic control in a smart city. The authors' goal was to reduce city traffic congestion and air pollution [13]. To manage the demands of intelligent grids, in [16], a renewable energy prediction program was designed based on artificial intelligence.

The use of artificial intelligence and optimization techniques has shown promising results in various healthcare applications [17–27], including the management of CVDs and related risk factors, offering a valuable tool for improving public health. For example, artificial neural networks (ANNs) have been used to elucidate the connections between olfaction, eating habits, and metabolic disturbances in the health of overweight patients [17]. Another study examined the prevalence of hypertension and obesity and studied markers of inflammation and oxidative stress using bioelectrical signal processing [18], while neural network models have been developed to predict cardiac and cardiovascular health by processing bioelectrical signals [19].

Artificial intelligence has also been used to improve model outcomes with deep learning (DL) algorithms by improving the prediction of CVD-related mortality and treatment

in patients with hypertension [20]. For example, the proposed model in [21] was trained on a broad dataset from the Korean National Health Information Database and achieved high accuracy in predicting CVD-related outcomes aiming to determine the relationship between CVD mortality and patients with hypertension.

Machine learning techniques have also been used for early the prediction and classification of CVD [22,23], as well as for the explicable detection of COVID-19 using chest radiographs [24]. In addition, studies have covered cardiovascular risk factors in obesity-related cardiovascular issues in Romanian children and adolescents using retrospective data analysis [25] and have examined the associations between multiple trajectories of BMI and waist circumference with blood pressure and hypertension in Chinese adults in a prospective study [26].

Similarly, the use of DL and device-assisted enteroscopy for automatic panendoscopy detection of erosions and ulcers is proposed. The study stakes the potential of deep learning to aid in the diagnosis of gastrointestinal disorders, including those that may contribute to the development of CVD [27].

1.1. Multiobjective Optimization

In multiobjective optimization, there are two main approaches, called a priori and a posteriori. The a priori method involves translating a multiobjective problem into a single-objective problem before obtaining a single solution. This is mainly performed using function weights to obtain a unique solution for the weight values. Using the a posteriori method, the result is obtained that the whole Pareto front (PF) contains a large number of non-dominated solutions [28,29]. In this way, common approaches to multiobjective optimization include:

- Goal attainment: decreases the values of a linear or nonlinear vector function with the mark values in a target vector; a weight vector indicates the objective's relative importance.
- Pareto front: based on detecting non-inferior solutions where a refinement in one objective affects another's degradation.

Several multiobjective optimization approaches are bio-inspired; a vast number are based on the Pareto front; therefore, in this a posteriori method, it is important for the technique to determine the suitable solution, and the most common approach is based on determining the knee region.

Bio-inspired multiobjective optimization algorithms have become a practical tool for deciphering situations with various objective functions [30]. The most representative bio-inspired algorithms are those rooted in particle swarms and evolution. Regarding the characteristics of the evolutionary scope, an appropriate approach to convey the optimal Pareto front (OPF) is accomplished by requiring multiple generations; on the contrary, algorithms based on particle swarms offer a high convergence rate; nevertheless, their main disadvantage is attaining proper diversity management [30,31].

In a multiobjective optimization problem, a non-dominated front is sought corresponding to the best values between the objectives [32]. A Pareto front is a region "knee" that has a noticeable convex bulge at the front and is essential for decision-making, and in most cases, it corresponds to an optimum balance.

Figure 1 displays widely known multiobjective optimization algorithms, an approach based on genetic algorithms [33–39], which is the most representative the family of non-dominated sorting genetic algorithms (NSGA); meanwhile, another approach is based on particle swarm [31,40–46], which is the most representative the family of algorithms' multiobjective particle swarm optimization (MOPSO).

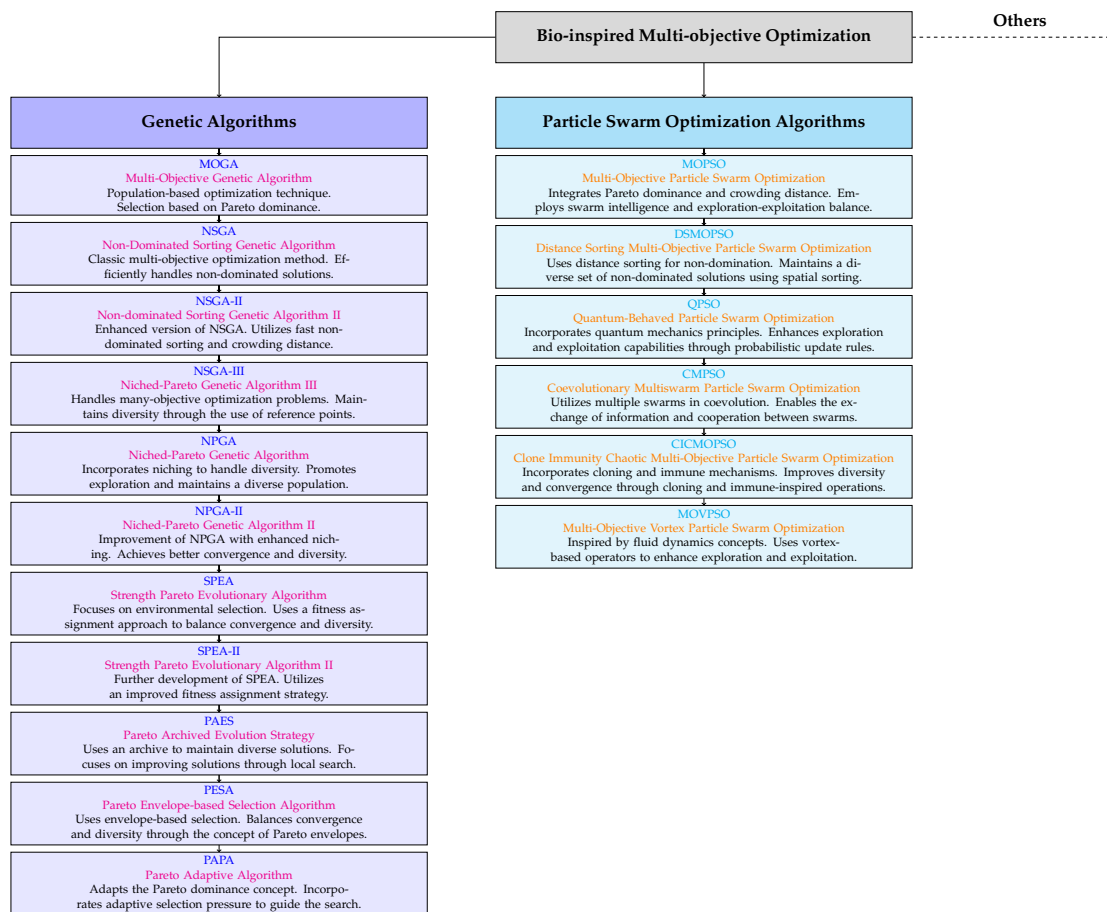


Figure 1. Most well-known multiobjective optimization algorithms.

1.2. Article Approach and Document Organization

The objective of this work is the proposal of a fuzzy logic system that allows the risk factor of suffering heart disease to be established. In this order, weight, age, gender, height, and systolic pressure are considered inputs, while the output is the cardiovascular risk (CVR) classification. Considering preliminary information on the inputs and, according to the literature, their effect on the CVR, the fuzzy logic system is proposed. As observed, the CVR output is based on preliminary information from the literature (allowing us to obtain simulated data). Therefore, to adjust the fuzzy logic system, a multi-objective approach is proposed, adding another output to the fuzzy logic system from which data are available and directly related to the CVR. This output corresponds to the BMI; then, to carry out the optimization process, real data from the BMI and previously simulated data from the fuzzy logic system are used to optimize the fuzzy model. In this way, when optimizing the system, the goal is to obtain a balance between the CVR and the BMI outputs. Finally, to determine the fuzzy system, the most appropriate configuration is chosen from the optimal Pareto front.

This proposal is made considering that, in objective optimization, if the functions are the same, the ideal point is reached; however, in the way that the objective functions are in conflict, they move away from the ideal value.

The article is structured as follows: Section 2 provides an overview of the concepts related to multiobjective optimization, focusing on the Pareto optimal front. Section 3 introduces the fuzzy system, and Section 4 discusses the implementation of multiobjective optimization. In Section 5, an analysis is conducted on the data acquired from the Pareto fronts, considering various aspects. Finally, Sections 6 and 7 present the discussion and conclusions of the research.

2. Multiobjective Optimization

Multiobjective design process optimization is applied in engineering, and, when balanced, it is essential in various objective functions. According to [30], the goal is to find a decision vector variable to fulfill some conditions and optimize a vector function.

The solution to a multiobjective optimization problem (MOP) consists of establishing a vector $\vec{x}^* = [x_1^*, x_2^*, \dots, x_n^*]^T$ that optimizes the vector objective formed by the functions in (1), also satisfying the m inequality constraints described in condition (2) and the p equality constraints contained in expression (3).

$$\vec{F}(\vec{x}) = [f_1(\vec{x}), f_2(\vec{x}), \dots, f_k(\vec{x})]^T \tag{1}$$

$$g_i(\vec{x}) \leq 0 \quad \text{for } i = 1, 2, \dots, m \tag{2}$$

$$h_i(\vec{x}) \leq 0 \quad \text{for } i = 1, 2, \dots, p \tag{3}$$

In Equation (1), the vector of variables $\vec{x}^* \in \Omega$ is a *feasible solution*, where the respective *feasible region* Ω is given by the constraints in Equations (2) and (3), which can be seen in the example shown in Figure 2, where there are two decision variables (with domain Ω) and two objective functions (with domain Λ) [30,47].

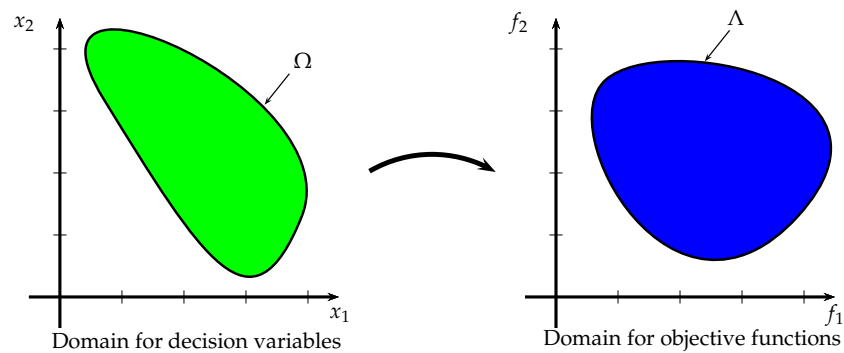


Figure 2. Domain of objective functions and decision variables.

2.1. Pareto Optimality Approach

In multiobjective optimization, an increase in a function performance commonly happens at the same time as a decrease in the remnant objective functions, which can be seen on the Pareto front.

According to the Pareto principle, if one solution dominates, it must be more effective in achieving at least one goal and never perform worse than the others [30,47–49]. As an example, solution R_1 in Figure 3 dominates solution R_2 since it is better in f_1 and f_2 . Nonetheless, it is not dominated by solution R_3 .

According to [30], a vector $\vec{x}^* \in \Omega$ is a Pareto optimum if another $\vec{x} \in \Omega$ is considered; then, $f_i(\vec{x}^*) \leq f_i(\vec{x})$ for all $i = 1, \dots, k$, and $f_j(\vec{x}^*) < f_j(\vec{x})$ for at least one j . Consequently, the set of vectors \vec{x}^* associated with the solutions are non-dominating; in this way, the collection of $f_i(\vec{x}^*)$ conforms to the OPF.

Meanwhile, according to [49], a point that minimizes each objective function corresponds to the ideal point $\vec{z}^{ideal} \in \mathbb{R}^m$, such as

$$\vec{z}_i^{ideal} = \min\{f_i(\vec{x}) | \vec{x} \in \Omega\}, \quad i = 1, \dots, m. \tag{4}$$

In addition, a utopian point $\vec{z}^{utopian} \in \mathbb{R}^m$ corresponds to an infeasible solution, where each component is

$$\vec{z}_i^{utopian} = \vec{z}_i^{ideal} - \epsilon_i, \quad i = 1, \dots, m, \quad \epsilon_i > 0. \tag{5}$$

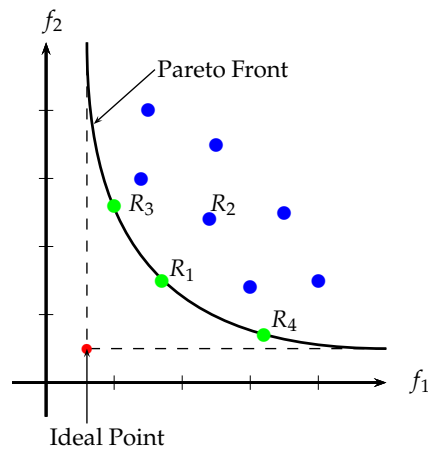


Figure 3. Optimal Pareto front and ideal point representation.

2.2. Multiobjective Performance Metrics

In multiobjective optimization, the performance metrics allow for establishing a comparison between different Pareto fronts.

According to [50,51], considering an actual Pareto front, it is mandatory to reduce the distance with the calculated Pareto front. Additionally, it requires a suitable distribution (in general uniform) of the vector solution. It is also necessary to extend the obtained non-dominated Pareto front. In this area, two relevant concepts are

- Diversity: Related to a number of solutions found.
- Convergence: Related to the quality of the solutions.

Regarding [52], for diversity, hypervolume is usually employed, and generational distance for convergence. This paper considers hypervolume as the performance metric.

2.3. Hypervolume Metric

The metric associated with hypervolume employs the quantity of the non-dominated volume in the space of objective functions as a diversity indicator. The metric of hypervolume estimates a multidimensional volume given a reference point. In Figure 4, an example is displayed for two objective functions.

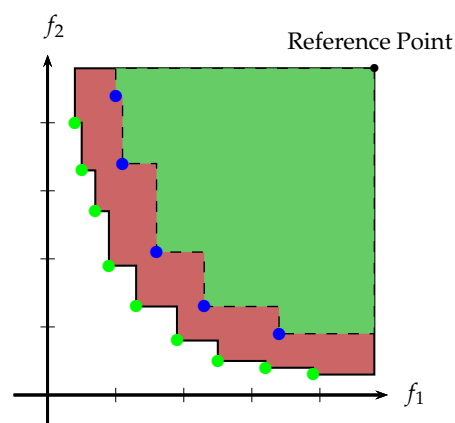


Figure 4. Graphical representation of hypervolume.

The hypervolume indicator obtains diversity and convergence in the multidimensional volume calculated with a Pareto front considering a reference point, as observed in Figure 4.

The hypervolume is defined on the Lebesgue measure Leb with a decision space R . The hypervolume metric $I_{HV}(A)$ for a set of solutions $A \subseteq R$ is calculated using a reference point $\vec{r} = (r_1, \dots, r_k) \in \mathbb{R}^n$ such that

$$I_{HV}(S) = Leb \left(\bigcup_{x \in S} [f_1(x), r_1] \times [f_2(x), r_2] \dots \times [f_n(x), r_n] \right) \tag{6}$$

in Equation (6) $[f_1(x), r_1] \times [f_2(x), r_2] \dots \times [f_n(x), r_n]$ represents the k -dimensional hypercube of all the points dominated by x [53].

2.4. Solution Selection Criterion

Multiobjective optimization encounters multiple sets of viable solutions considering the restrictions established by the designer. Conversely, for actual implementation, only one solution is required. Thus, the most suitable solution can be selected in various ways [54–56]. For example, in [57] an iterative Pareto fuzzy method is proposed to determine a suitable balance between all objective functions. Another possible approach to determine an adequate solution can be based on the Pareto optimal front’s clustering process, considering the analysis presented in [47].

The most common approach to determining a suitable solution is based on determining the knee points. In this way, it seeks to have a balance between the objectives to be optimized. Different approaches are proposed to determine the knee solutions, as observed in [54–56]. One of the most common is the one based on Euclidean metrics, since it is the most intuitive possible distance examination between any two points [56]. In conclusion, by finding a result using the multidimensional Euclidean metrics method, it is possible that it becomes a compromise between the objective functions [56]. For the analysis of non-dominated solutions, the Euclidean metrics correspond to the following:

$$d(R, K) = \sqrt{\sum_{i=1}^N |R_i - K_i|^2} \tag{7}$$

where R is the reference point, one of the most commonly used as the one ideal point; K is a solution in the Pareto front; R_i and K_i are the respective components of R and K ; and finally, N is the number of components of K . Figure 5 displays the concept of Euclidean distance considering the ideal point.

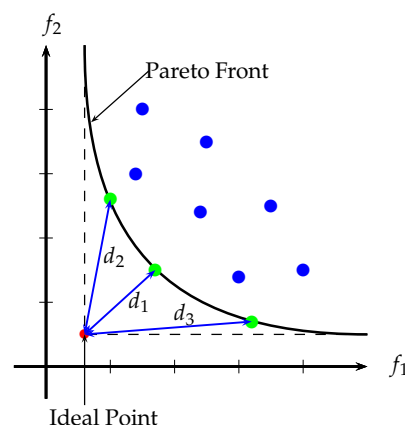


Figure 5. Graphical representation of Euclidean distance considering the ideal point.

3. Proposed Fuzzy System

Mamdani-type fuzzy logic systems are a type of fuzzy inference system used to model complex and nonlinear systems. These systems use fuzzy sets in both input and output universes and rely on linguistic rules to perform inference.

The input of a Mamdani-type fuzzy logic system is usually a numerical value coming, for example, from a sensor. For this value to be processed by the fuzzy system, a membership is assigned to each of the fuzzy sets that constitute the input universe.

The Mamdani-type fuzzy inference system uses linguistic rules to make inferences and produce a fuzzy output. Each linguistic rule consists of a premise and a conclusion. The premise is a linguistic expression describing the conditions in which the rule applies, while the conclusion is a linguistic expression describing the action to be taken if the premise is satisfied [58].

Linguistic labels play a crucial role in fuzzy systems, allowing them to handle the uncertainty and vagueness of data. A linguistic variable is a variable whose values are words or sentences in a natural or artificial language [59,60]. These words or sentences are associated with fuzzy sets defined by membership functions that assign degrees of membership to each element in the universe of discourse. The membership functions can be defined in various ways, such as triangular, trapezoidal, or Gaussian, depending on the shape of the fuzzy set. The linguistic labels associated with the fuzzy sets are used to represent the degree of truth or falsity of a proposition and to make decisions based on uncertainty or incomplete information.

Approximate reasoning is viewed as a process of approximate solution of a system of relational assignment equations. This process is formulated as a compositional rule of inference that includes modus ponens as a special case [60]. The effectiveness of fuzzy systems depends on the quality of the linguistic labels and the membership functions used to define the fuzzy sets. Tang and Zheng proposed a new linguistic modeling technique based on the semantic similarity relation among linguistic labels [61]. This method can be applied in complex systems that do not directly rely on fuzzy sets to model the meaning of natural language.

Fuzzy logic can be used as an expert system in the medical diagnosis and treatment of heart disease by allowing the incorporation of uncertainties and the representation of imprecise variables, as displayed in [62]. Although the authors do not employ an optimization process to fit the fuzzy system, this study can be considered as a reference.

For the case under consideration, the expert system for medical diagnosis of cardiovascular risk (heart disease) can be designed using fuzzy logic as follows:

1. Identify symptoms and signs of heart disease used as input to an expert system. This information can include blood pressure, cholesterol levels, heart rate, family history, and lifestyle.
2. Determine the degree of membership of each symptom or character using fuzzy membership functions.
3. Define rules of inference that describe how different symptoms and signs combine to arrive at a diagnosis. These rules can be heuristic or knowledge-based.
4. Use fuzzy reasoning to evaluate each input symptom or sign and determine its membership in each possible heart disease class.
5. Sum the results of the inference to obtain an estimate of the probability that the patient meets all possible categories of heart disease.
6. Select the most likely heart disease category and present it to the user as the most likely diagnosis [62].

It is important to remark that fuzzy logic is not the only approach to the medical diagnosis of heart disease but can be a valuable tool when combined with other methods and the expertise of a specialized physician [63].

The fuzzy logic system presented aims to determine an individual's body mass index and the risk of cardiovascular disease, using as input several variables related to weight, age, gender, height, and systolic blood pressure.

The system is defined through a fuzzy inference system (FIS) structure in MATLAB created with the "newfis" function. The input and output variables are then included with the "addvar" function, and the membership functions of each variable are specified using the "addmf" function.

3.1. Input Parameters

The proposed system helps determine if a person is at risk for heart problems by considering the inputs weight, age, gender, height, and systolic pressure. In this way, to perform the multiobjective optimization process, one output is the cardiovascular risk classification, and the other corresponds to the body mass index. As can be seen, important aspects related to health, such as weight, age, height, gender, and blood pressure in heartbeats, are considered. Weight and height help figure out the BMI, which is very important to determine health related to weight. Systolic blood pressure is a way to check heart health. Doctors use it, along with age, sex, and height, to see if a person might have heart problems in the future. This fuzzy logic system checks many things to see if a person is healthy.

3.1.1. Weight

Excess weight, particularly excess visceral fat and fat accumulation in lean tissues, mainly defines the threat of cardiovascular issues in overweight or obese individuals. Maintaining a healthy weight is essential for preventing cardiovascular disease and improving overall health [64]. The following ranges were used in the proposed fuzzy logic system:

- Between 15 to 30 kg;
- Between 31 to 45 kg;
- Between 46 to 60 kg;
- Between 61 to 75 kg; and
- Over 76 kg.

3.1.2. Age

Aging is associated with the progressive degeneration of the heart and blood vessels, making them more vulnerable to stressors, contributing to increased cardiovascular morbidity and mortality in the older population, which are especially prevalent in older adults. Those over 65 years of age are at a high risk of atrial fibrillation and related stroke, while approximately 20% of people over 80 years of age are at risk of heart failure [65].

The following ranges were used in the proposed fuzzy logic system:

- Under 20 years old;
- Between 20 to 35 years old;
- Between 36 to 49 years old;
- Between 50 to 60 years old; and
- Over 60 years old.

3.1.3. Gender

Gender is a critical factor determining cardiovascular health, yet it has been largely neglected. Cardiovascular disease trajectories and outcomes differ by biological sex and, in turn, define cardiovascular health from conception through early childhood, when health behaviors and risk factors are established through adolescence until adulthood [66]. In this order, the gender tag corresponds to:

- Female and
- Male.

3.1.4. Height

Height is important in determining BMI, and, in turn, BMI is a leading risk factor for cardiovascular disease. It is necessary to consider both the mortality and the morbidity associated with excess weight in the assessment of disease burden [67]. The following ranges were used in the proposed fuzzy logic system:

- Between 0.90 to 1.30 m;
- Between 1.31 to 1.50 m;
- Between 1.51 to 1.65 m;

- Between 1.66 to 1.80 m; and
- Over 1.80 m.

3.1.5. Systolic Pressure

High isolated systolic hypertension or systolic blood pressure prevails in older adults and represents a significant threat for chronic kidney disease, coronary artery disease, and stroke. There is a direct relationship between these complications and elevated systolic BP, independently of sex or ethnicity. However, it worsens, given that individuals grow old and have comorbidities, as demonstrated in two extensive prospective studies in more than one million subjects [62,68]. The following ranges were used in the proposed fuzzy logic system:

- Normal;
- High;
- Hypertension level one;
- Hypertension level two; and
- Hypertension crisis.

3.2. Output Parameters

This system looks at two aspects to see if a person is healthy. BMI helps us know if individuals have a healthy weight based on height. Cardiovascular disease risk is how likely someone is to acquire diseases that affect the heart, including high blood pressure, coronary heart disease, and stroke. This system helps doctors and health workers make better decisions about patient care by using information about body weight and heart health.

3.2.1. Body Mass Index

BMI, or body mass index, refers to a measure used to assess obesity and overweight in adults. If the patient has a high BMI condition, it means that they have a BMI above a healthy level, which can have negative health consequences. BMI is estimated by dividing a person's weight in kilograms by the square of their height in meters. Therefore, it is a measure that considers both a person's weight and height to determine if they are in a healthy range [69]. The following ranges were used in the proposed fuzzy logic system:

- Normal weight;
- Pre-obesity;
- Class 1 obesity;
- Class 2 obesity; and
- Class 3 obesity.

3.2.2. Classification

Risk factors for cardiovascular disease are those aspects that increase the probability of developing cardiovascular disease, particularly coronary heart disease. Some of the most common risk factors are as follows:

- Age: CVD risk increases with age.
- Gender: men carry a higher risk than women before menopause. After menopause, the risk in women is equal to that of men.
- Family history: if a close family member has suffered from cardiovascular disease, the risk increases.
- Tobacco: smoking is a key factor for cardiovascular disease.
- Hypertension: high blood pressure can damage arteries and raise the risk of coronary diseases.
- Diabetes: individuals with diabetes have an increased risk of cardiovascular disease.
- High cholesterol: high levels can increase the risk of coronary heart disease.
- Obesity: overweight and obesity increase the risk of cardiovascular disease.

- Physical inactivity: lack of physical activity is also a booster of cardiovascular disease risk.
- Stress: if prolonged, stress increases the probability of cardiovascular complications.

It is necessary to point out that many of these risk factors are modifiable and can be prevented or controlled with lifestyle changes, such as no smoking habits, regular physical activity, control of cholesterol and blood pressure, reduction in stress levels, and healthy nutritional habits [70]. The following ranges were used in the proposed fuzzy logic system:

- Very low risk;
- Low risk;
- Moderate;
- High risk; and
- Very high risk.

To design the fuzzy system, various aspects can be considered, as presented in the literature [71], such as the ranges for input and output variables. Figure 6 displays the scheme associated with the proposed fuzzy system. The two outputs share the fuzzy sets of the inputs and the rule set and are independent of the fuzzy sets of the outputs.

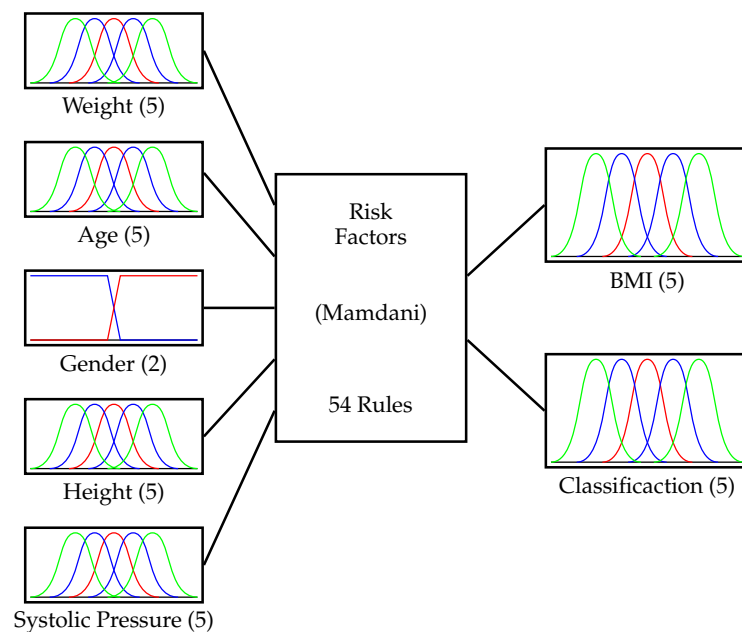


Figure 6. Scheme associated with the proposed fuzzy system.

3.3. Fuzzy Rules

The fuzzy logic system is based on inference rules that allow conclusions to be drawn from fuzzy premises. The table of inference rules shows the possible combinations of input values and the corresponding outputs obtained by applying the inference rules. These rules are designed to work with fuzzy values, i.e., values that are not simply true or false but may have intermediate degrees of belonging to a given set. The table of inference rules makes it possible to establish the output corresponding to a particular combination of input values, which facilitates the decision making and control of complex systems involving multiple fuzzy variables (see Table A1).

3.4. Dataset

The research used as a source of information for the study was a dataset on medical care in Colombia in 2018, which includes information on the number of people who received medical care in different types of health facilities, such as public, private, and mixed. It also includes data on the number of consultations, procedures, and hospitalizations that took place that year, including people of different ages, genders, and health conditions.

This dataset was used to analyze the performance of the health system and to identify patterns related to cardiovascular disease. The study used a multiobjective approach for the optimization of a fuzzy system for the classification of cardiovascular risk and body mass index based on a subset of the dataset. Specifically, the study analyzed 200 records from the dataset, taking as input data the age, sex, weight, height, and systolic blood pressure of the patients in the database and as output their body mass index [72].

The database can be used in data analysis or in the creation of predictive models in health care. To use this database, it was necessary to perform a cleaning and transformation process to adapt the data to the proposed analysis tool [72].

The following is the total number of columns presented by the dataset for a total of 43 items (columns in the raw data).

- | | | |
|----------------------------------|-----------------------------|-----------------------------|
| 1. Document | 16. Date born | 31. Pharmacological history |
| 2. Age | 17. City database | 32. Civil state |
| 3. Date | 18. External cause | 33. Rh |
| 4. Weight | 19. Reason for consultation | 34. Chronic decripcion |
| 5. Sex | 20. Symptom.Resp | 35. Chronic |
| 6. Size | 21. Planned | 36. Diagnosis Dx exit |
| 7. Fcard | 22. T.pregnancy | 37. User type |
| 8. Diagnosis | 23. F.U.R | 38. Oximetry |
| 9. Fresp | 24. Zone | 39. Revision of cytology |
| 10. Description of the diagnosis | 25. B.M.I | 40. Breast lactation |
| 11. Temp | 26. Systemic Tension | 41. Tsh |
| 12. Is out | 27. Diastolic tension | 42. Uterine height |
| 13. Initial service unit | 28. TebsMedia | 43. Cephalic Perimeter |
| 14. Join. serv. final | 29. pregnant | |
| 15. Entity | 30. Weeks of gestation | |

4. Multiobjective Optimization Process

The implementation is performed using the respective libraries of MATLAB (2017a) of fuzzy logic and MOEAS. It employed a PC Lenovo IdeaPad 5 14ITL05 with an 11th Gen Intel Core i7-1165G7 processor 2.80 GHz, with 16.0 GB of RAM, and Windows 10.

The database employed in the optimization process is taken from [72]. The input data used are shown in Figure 7 and the output data in Figure 8; 80% of the data are used for optimization and the remaining 20% are employed for validation.

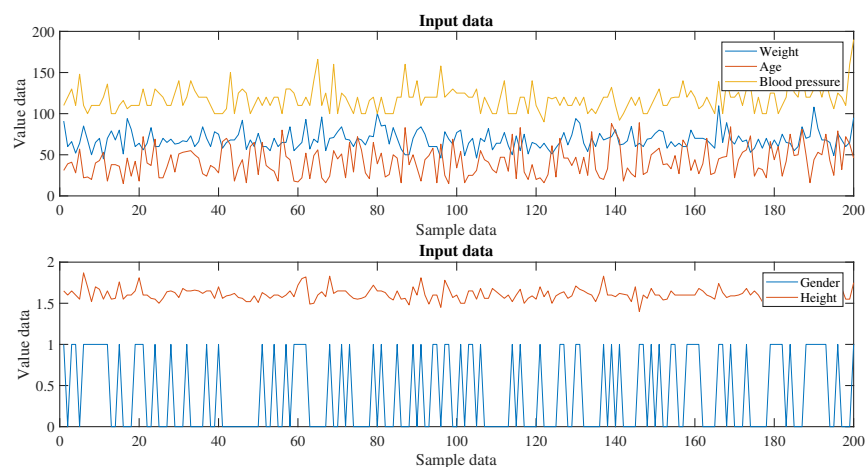


Figure 7. Input data used.

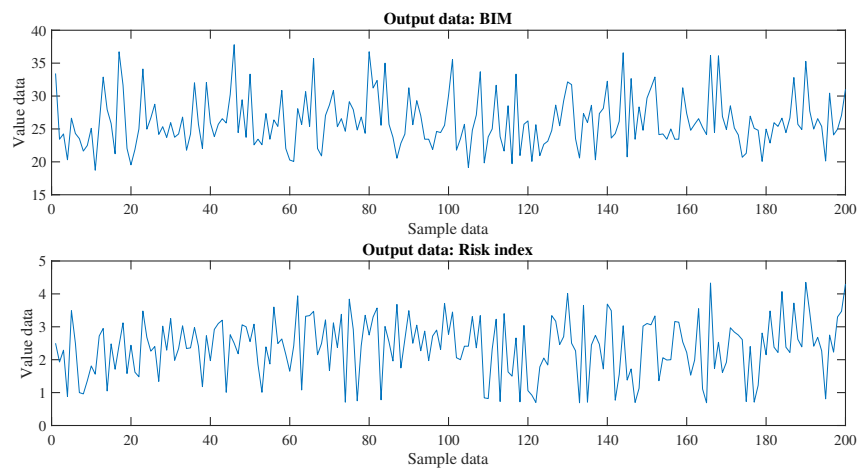


Figure 8. Output data used.

With data displayed in Figures 7 and 8, the two objective functions are established as follows:

$$f_1 = \frac{1}{N} \sum_{i=1}^N (r_1(i) - y_1(x(i)))^2 \quad (8)$$

$$f_2 = \frac{1}{N} \sum_{i=1}^N (r_2(i) - y_2(x(i)))^2 \quad (9)$$

where r_1 and r_2 are the reference data, y_1 and y_2 are the output of the fuzzy system for a input data $x(i)$, and N is the total data employed.

The variables to be optimized correspond to the parameters of the fuzzy sets; it is worth noting that the set of rules is not modified, since it corresponds to the preliminary knowledge of the system. In the same way, the fuzzy sets associated with the gender of the person are not modified since the data only contain male and female gender.

The implementation in MATLAB is conducted with the function “*gamultiobj*”, which employs a variation in the NSGA-II, a controlled elitist genetic algorithm. An elitist GA favors individuals with more suitable fitness values (rank). Furthermore, a controlled elitist GA chooses individuals to expand the population diversity even when they display a lower fitness value. The bound constraints $lb \leq x \leq ub$ are given by the ranges of the fuzzy sets in the respective input or output [73].

Considering the stochastic behavior of the optimization algorithm, 20 executions of the optimization process are performed. According to [74–78], a significant parameter of NSGA-II is the population size; therefore, for the implementation of the multiobjective algorithm, a different population size is considered. According to the guidelines of [73], the population can be taken between 50 and 200. The configurations from the MOEA are as follows:

- Configuration 1: Population 100.
- Configuration 2: Population 150.
- Configuration 3: Population 200.
- Configuration 4: Population 250.

The rest of the algorithm’s parameters are set according to the suggestion displayed in [73]. In this order, the value parameters are as follows:

- Iterations: 4000.
- Crossover Fraction: 0.8.
- Elite Count: $0.05 \times$ Population Size.
- Function Tolerance: 1×10^{-8} .
- Migration Fraction: 0.2.

- Mutation Function: Mutation Adapt Feasible.

The first result to observe consists of the processing time used to perform the optimization (20 executions) of each configuration. A statistical summary of the results obtained can be seen in Table 1. It can be seen that as the population increases, the processing time also increases. It should also be noted that the total time used was 323.0122 h, namely 13.4588 days.

Table 1. Statistical summary of the processing time (in hours).

Configuration	Conf. 1	Conf. 2	Conf. 3	Conf. 4
Maximum	2.3519	3.5076	4.6794	5.8378
Minimum	2.2796	3.4124	4.5598	5.6504
Average	2.3140	3.4601	4.6119	5.7646
Variance	1.0079	1.8262	3.4650	10.8134
Total	46.2807	69.2019	92.2381	115.2915

The reference point used to calculate the hypervolume is obtained by determining the maximum values of f_1 and f_2 obtained for all the Pareto fronts of all the configurations considered. In this way, a general reference point is achieved for all the results obtained. Table 2 displays the statistical summary of the hypervolume value for each Pareto front obtained. The highest value of hypervolume is obtained in configuration 2; however, on average, the highest value is found in configuration 4. In the same way, for the lowest value obtained for hypervolume, configuration 4 presents the highest value. In this way, an adequate solution of the Pareto front can be found in the results of configuration 2 or 4.

Table 2. Statistical summary of the hypervolume value for each Pareto front obtained.

Configuration	Conf. 1	Conf. 2	Conf. 3	Conf. 4
Maximum	12.3275	12.4299	12.3041	12.4237
Minimum	8.2692	9.3182	8.6107	9.4830
Average	9.8659	10.5693	10.4517	10.7733
Variance	0.9197	0.7143	1.1097	0.8062

5. Result Analysis

This section displays the results from the multiobjective optimization process. First, it presents the optimal Pareto front obtained and then the results obtained for the best cases of f_1 and f_2 ; then, an analysis is carried out focusing on having the best balance between f_1 and f_2 .

In order to determine the best Pareto front, the best responses obtained from all the executions are combined, Figure 9 shows the optimal Pareto front obtained. These figures show the result using the data for optimization (from 0 to 160) and the validation data (from 161 to 200).

From the optimal Pareto front obtained, as an interesting result, the best configuration obtained for f_1 and f_2 is presented separately. Figure 10 displays the best configuration for f_1 , obtaining $\vec{F} = [2.0589, 0.3112]$; meanwhile, in Figure 11, the best result for f_2 is displayed where $\vec{F} = [5.1022, 0.1855]$. With these results and figures, it is possible to observe the best values that can be obtained for each objective function and, therefore, for each output of the fuzzy logic system.

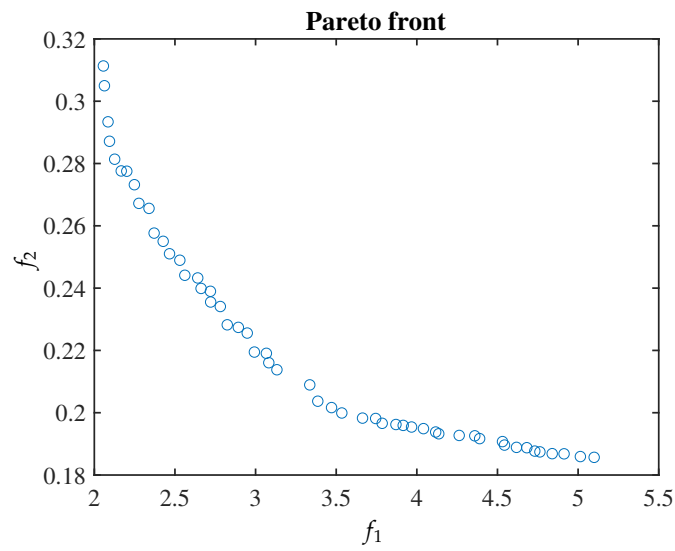


Figure 9. Optimal Pareto front obtained.

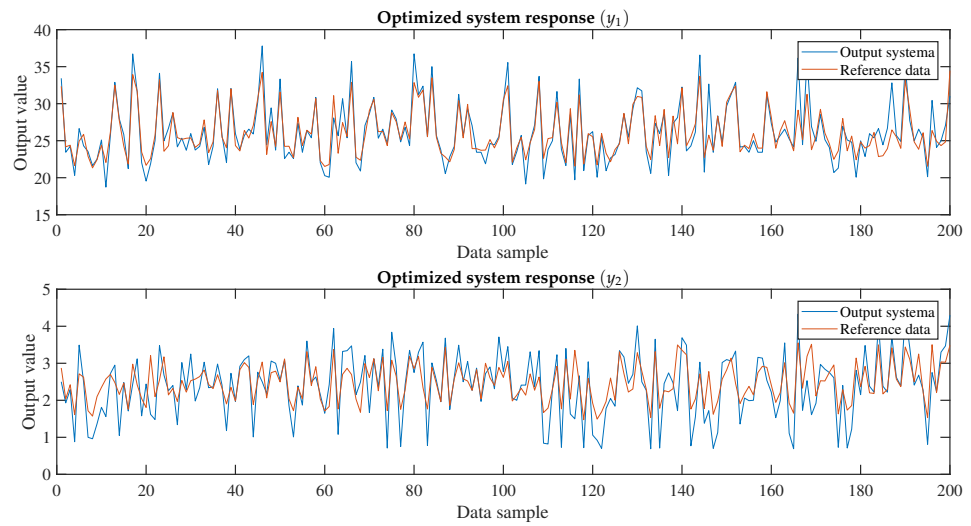


Figure 10. Simulation result for the best configuration for f_1 .

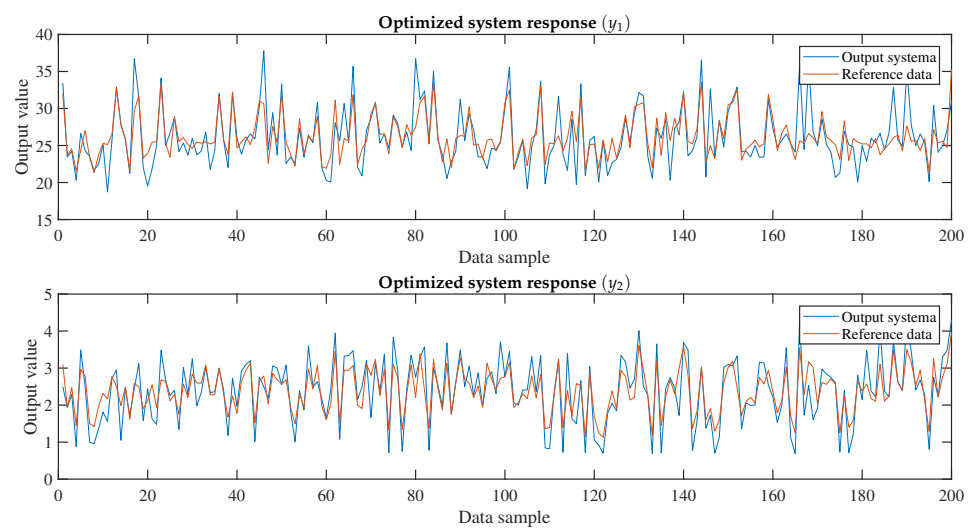


Figure 11. Simulation result for the best configuration for f_2 .

5.1. Fuzzy System Selection

The configuration that gives the balance between f_1 and f_2 is obtained considering the distance from the ideal point and the optimal Pareto front.

In order to select the suitable configuration for the fuzzy system, the shortest distance is considered between the ideal point and the optimal Pareto front, as is shown in Figure 12.

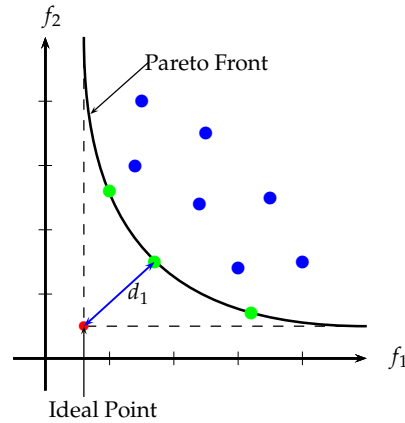


Figure 12. Shortest distance between the ideal point and the optimal Pareto front.

In this case, $\vec{F} = [2.0589, 0.3112]$ is obtained; Figure 13 displays the simulation obtained with the configuration that exhibits the shortest distance from the ideal point of the Pareto optimal front. As can be appreciated in these results, with the selected solution, it is possible to have a balance between the two objective functions and, therefore, for the outputs of the fuzzy logic system.

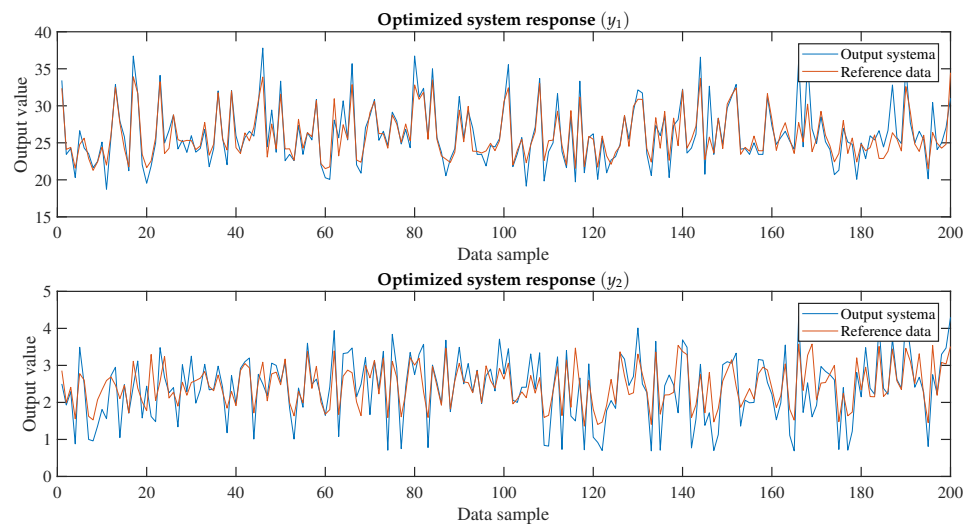


Figure 13. Simulation result for the best configuration for the knee point of the Pareto optimal front.

5.2. Fuzzy System Interpretability

The interpretability of the configuration of fuzzy sets for input variables is presented in five figures, each of which represents the fuzzy sets for a different input variable. In this way, given the location and shape of the fuzzy set, a linguistic label can be assigned.

When analyzing Figure 14, it can be seen that there are five fuzzy sets defined for weight, and the membership function of each fuzzy set indicates how values are assigned to each linguistic label. In this way, it can be observed that sets W_1 and W_5 are located in the same place with a very similar amplitude that can be related to mean values, while fuzzy set W_2 is associated with low values and set W_3 with high values. Intermediate values are associated with W_1 , W_5 , and W_4 . These labels allow for a linguistic relationship among the

input variables (risk factors for cardiovascular diseases) and the value of the body mass index with the risk factor that a person would have for developing cardiovascular disease.

The input of age in Figure 15 can be defined as the linguistic labels for the respective fuzzy sets; it is evident that sets A_1 and A_2 coincide in the same place and amplitude (representing the same concept). Similarly, set A_5 can be associated with low values, in contrast to set A_3 , which can represent higher values, and finally, set A_4 with intermediate values.

Considering Figure 16 associated with the input of gender, according to the data available, two linguistic labels corresponding to masculine and feminine genders are considered. Since these two sets are well established during the optimization process, their parameters are not modified.

Finally, considering the inputs in Figures 17 and 18, the configurations are displayed for the inputs of height and systolic blood pressure, respectively. Considering linguistic labels, it is observed that in height, set H_5 presents high values, H_2 presents low values, and intermediate values are presented in H_3 , H_1 , and H_4 . Similarly, in systolic blood pressure, there is a tendency towards intermediate values with sets P_4 , P_3 , and P_2 , which also share a similar value and amplitude, and a high-value label for P_5 and a medium-high value with P_1 are also observed.

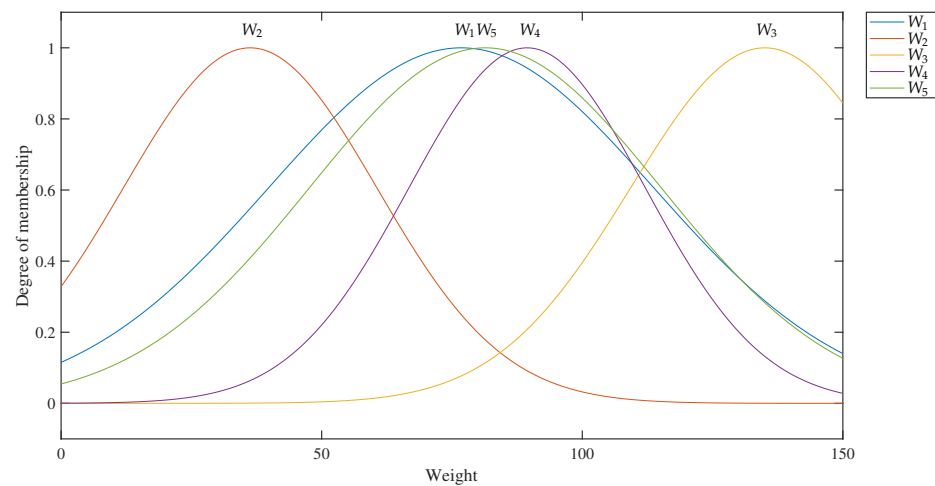


Figure 14. Configuration of the fuzzy sets for the weight input.

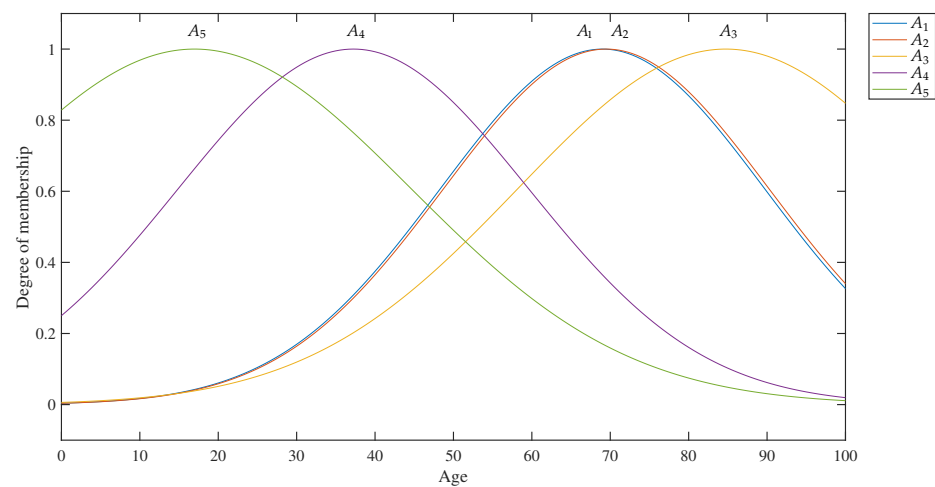


Figure 15. Configuration of the fuzzy sets for the age input.

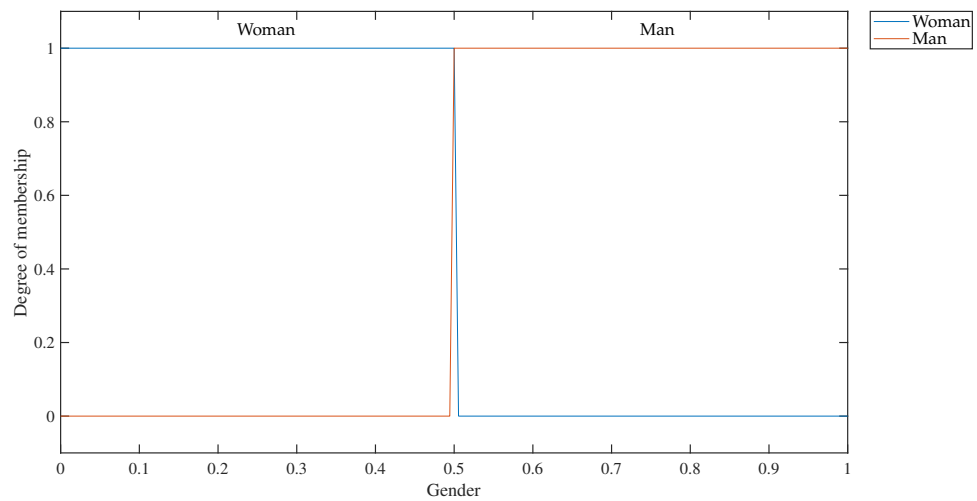


Figure 16. Configuration of the fuzzy sets for the gender input.

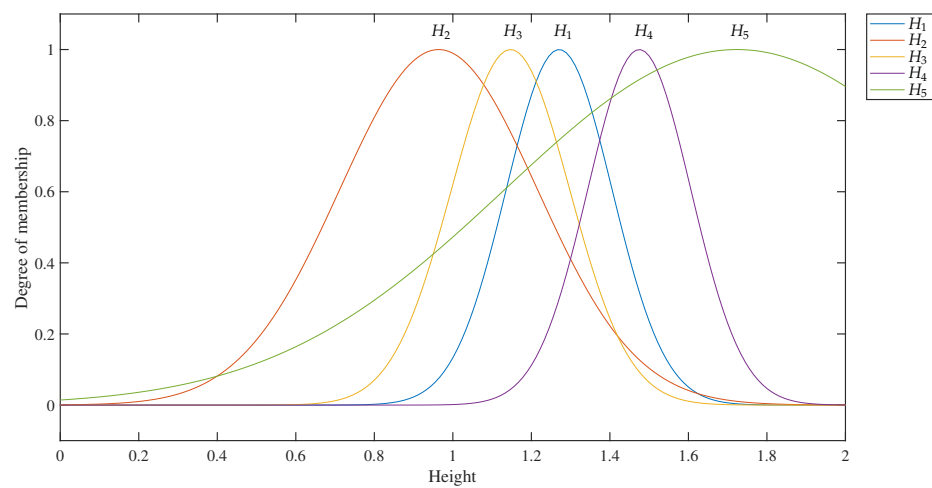


Figure 17. Configuration of the fuzzy sets for the height input.

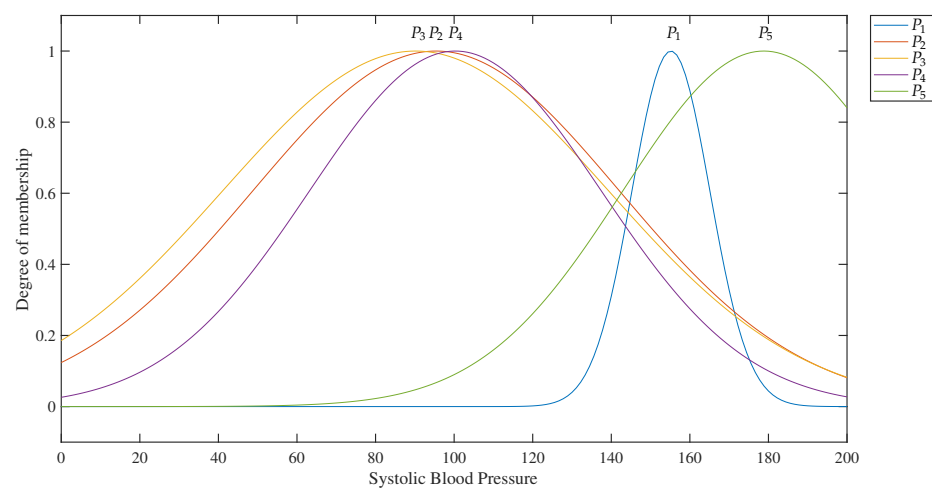


Figure 18. Configuration of the fuzzy sets for the systolic blood pressure.

Next, the same interpretability is made on the outputs obtained in such a way that the fuzzy set configurations in Figures 19 and 20, respectively, are obtained. In this order, the results are analyzed as follows: for y_1 , the body mass index has the highest value in the I_3

set, as well as in I_5 , while I_4 has an intermediate value, and I_2 and I_3 have low values but with a large amplitude.

Similarly, for the configuration of y_2 related to the risk factors for cardiovascular disease, it is observed that C_2 shows a low value, while C_1 and C_5 maintain their high values, and C_4 and C_3 display intermediate values and the same amplitude. This way, the interpretability of these fuzzy sets is obtained considering different linguistic labels.

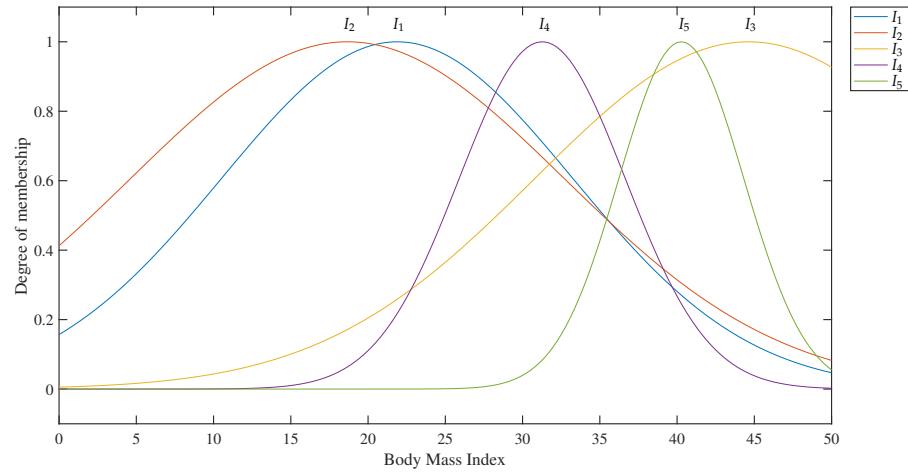


Figure 19. Configuration of the optimized fuzzy sets for the output y_1 .

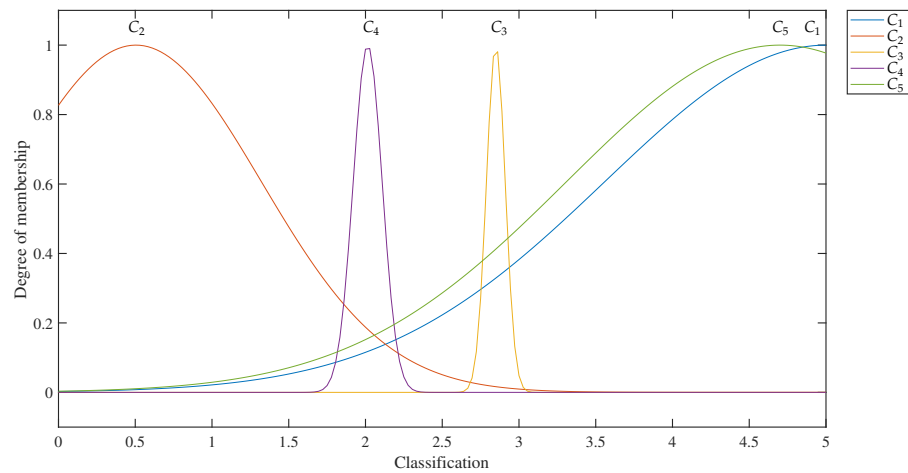


Figure 20. Configuration of the optimized fuzzy sets for the output y_2 .

As can be seen in these results, in most cases, a suitable distribution of the fuzzy sets is achieved in the respective universes of discourse in such a way that it is possible to establish a linguistic label for each fuzzy set. This allows adequate interpretability of the fuzzy logic system.

Regarding fuzzy medical-linguistic results, it is observed that fuzzy sets C_1 and C_5 are close and indicate a high risk factor for cardiovascular disease. On the other hand, the sets C_2 , C_3 , and C_4 are distributed in the rest of the output discourse universe covering different sectors, where C_3 and C_4 can be associated with middle risk and C_2 with low risk. A more thorough study of the gathering of fuzzy linguistic medical outcomes can be made using clustering algorithms from the data output on the fuzzy system.

6. Discussion

This proposal enables a system adjustment in cases where real data are not available for one of the outputs of the fuzzy system used for multiobjective optimization. This process is suitable when there is a direct relationship between the output with real data

and the output that lacks them. For example, the relationship between elevated BMI and an increased risk of cardiovascular disease are considered.

It is important to note that the proposal aims to strike a balance between the output with real data and the one with simulated data. Multiobjective optimization enables the generation of a wide range of solutions that exhibit different relationships between the two outputs under consideration.

The proposed strategy seeks to ensure that the two outputs exhibit similar behavior so that a balance can be achieved between the output with real data and the output with simulated data during the optimization process. The two outputs share the fuzzy sets of the inputs and rule sets, and they are independent of the fuzzy sets of the outputs. This approach allows for the simultaneous adjustment of common parts between the two outputs and provides flexibility in adjusting these outputs.

Another aspect to consider concerns studies such as [6–8], where it is stated that the BMI is not the best measure of health. Despite some controversy over BMI as an exclusive factor in health assessment, in this paper it is employed as a reference to adjust the fuzzy system. As an alternative, in future work, another index to carry out the optimization process can be considered.

It should be noted that although the optimization of the fuzzy logic system spends an average of 5.7646 h (configuration 4; see Table 1) after the fuzzy system has been optimized, it can be used to classify the risk of cardiovascular disease. If it is necessary to perform a new adjustment of the fuzzy system, the best configuration of the multiobjective algorithm can be used to optimize the fuzzy logic system again.

Finally, to improve the performance of the model and the optimization process, a clustering process can be incorporated in different instances, such a

1. The preliminary configuration of fuzzy sets and thus a determination of a suitable number of sets to use. This also can be used to set the constraints and population of the genetic multiobjective optimization algorithm.
2. Study of the grouping of fuzzy medical-linguistic results on cardiovascular risk. This can be employed to improve the interpretability of the fuzzy sets and rules of the CVR system.

7. Conclusions

The fuzzy logic system was fine-tuned using multiobjective optimization, allowing for the use of real data to fit y_1 (body mass index) and simulated data for y_2 (risk factor classification). By proposing this system, the aim is to assist individuals in identifying risk factors for heart disease while also promoting the awareness of healthy habits to prevent this condition.

The selection of an appropriate configuration for the fuzzy system is achieved by minimizing the distance between the utopian point and the Pareto optimal front. However, after the optimization process, it is crucial to ensure the interpretability of the fuzzy logic system, as the stochastic nature of the genetic algorithm may result in configurations with low interpretability.

The use of multiobjective optimization and Pareto dominance allowed us to obtain a set of optimal solutions that represent the best possible balance between two competing objectives: the accuracy of the real BMI data and the accuracy of the simulated CVD risk data. Using a controlled genetic algorithm was a suitable choice for this problem, as it allowed us to efficiently explore the solution space and obtain consistent results in different settings.

This study underscores the value of applying multiobjective optimization algorithms to develop better BMI management strategies and improve overall cardiovascular health outcomes.

The implementation of the optimized fuzzy logic system can be of great use in the classification of body mass index and cardiovascular disease risk in the medical field, as it

allows a better approximation of real and simulated data, which in turn can help to make more informed decisions about the patient’s health.

The proposed model utilizing fuzzy logic and optimization algorithms presents a suitable approach to identifying and mitigating risk factors for cardiovascular diseases. The significance of this work lies in its potential to improve personalized health outcomes and reduce the incidence of CVD globally.

In future work, rule optimization could be carried out, and data from expert surveys could be used to evaluate the system’s performance.

Author Contributions: Conceptualization, H.C.V., H.E.E. and L.A.B.; Methodology, H.C.V., H.E.E. and L.A.B.; Project administration, H.C.V., H.E.E. and L.A.B.; Supervision, H.E.E.; Validation, H.C.V.; Writing—original draft, H.C.V., H.E.E. and L.A.B.; Writing—review and editing, H.C.V., H.E.E. and L.A.B. All authors have read and agreed to the published version of the manuscript.

Funding: This research received no external funding.

Institutional Review Board Statement: Not applicable.

Informed Consent Statement: Not applicable.

Data Availability Statement: The data used can be requested from the authors.

Acknowledgments: The authors express gratitude to the Universidad Distrital Francisco José de Caldas.

Conflicts of Interest: The authors declare no conflict of interest.

Appendix A. Fuzzy System Rules

In this appendix Table A1 is displayed, which contains the inference rules. This table displays the combinations of inputs and the corresponding outputs associated with the inference rules.

Table A1. Inference rules for the proposed system.

Input		Output				
Weight	Age	Gender	Height	Systolic Pressure	BMI	Risk Classification
From 15 to 30 kg	Under 20 years	Female	-	Normal	Normal weight	Very low risk
From 31 to 45 kg	From 20 to 35 years	Male	-	Normal	Normal weight	Very low risk
From 46 to 60 kg	From 36 to 49 years	Female	From 1.51 to 1.65 m	High	Pre-obesity	Low risk
From 61 to 75 kg	From 50 to 60 years	Male	From 1.66 to 1.80 m	Hypertension level one	Class 1 obesity	Moderate
Over 76 kg	Over 60 years	Male	Over 1.80 m	Hypertension level two	Class 2 obesity	High risk
From 46 to 60 kg	From 36 to 49 years	Female	From 1.51 to 1.65 m	Hypertension crisis	Class 3 obesity	Very high risk
From 31 to 45 kg	From 20 to 35 years	Female	-	Hypertension level one	Pre-obesity	Moderate
From 61 to 75 kg	From 50 to 60 years	Male	-	Hypertension level two	Class 2 obesity	High risk
Over 76 kg	Over 60 years	Female	-	Hypertension crisis	Class 3 obesity	Very high risk
From 15 to 30 kg	Under 20 years	Female	From 1.31 to 1.50 m	Normal	Normal weight	Very low risk
From 15 to 30 kg	Under 20 years	Female	From 1.31 to 1.50 m	High	Pre-obesity	Moderate
From 15 to 30 kg	Under 20 years	Female	From 1.31 to 1.50 m	Hypertension level one	Pre-obesity	Low risk
From 15 to 30 kg	Under 20 years	Female	From 1.31 to 1.50 m	Hypertension level two	Class 1 obesity	High risk
From 15 to 30 kg	Under 20 years	Female	From 1.31 to 1.50 m	Hypertension crisis	Class 2 obesity	Very high risk
From 31 to 45 kg	Under 20 years	Female	From 0.90 to 1.30 m	Normal	Normal weight	Very low risk
From 46 to 60 kg	Under 20 years	Male	From 0.90 to 1.30 m	High	Pre-obesity	Low risk
From 61 to 75 kg	Under 20 years	Female	From 0.90 to 1.30 m	High	Class 2 obesity	Moderate
From 15 to 30 kg	Under 20 years	Female	From 0.90 to 1.30 m	Normal	Normal weight	Very low risk
From 31 to 45 kg	From 20 to 35 years	Female	From 0.90 to 1.30 m	High	Pre-obesity	Low risk
From 31 to 45 kg	From 36 to 49 years	Male	From 1.31 to 1.50 m	High	Pre-obesity	Low risk
From 46 to 60 kg	From 36 to 49 years	Female	From 1.31 to 1.50 m	Hypertension level one	Class 1 obesity	Moderate
From 61 to 75 kg	From 36 to 49 years	Male	From 1.31 to 1.50 m	Hypertension level two	Class 2 obesity	High risk

Table A1. Cont.

Input			Output			
Weight	Age	Gender	Height	Systolic Pressure	BMI	Risk Classification
Over 76 kg	From 36 to 49 years	Female	From 1.31 to 1.50 m	Hypertension crisis	Class 3 obesity	Very high risk
From 15 to 30 kg	From 50 to 60 years	Male	From 1.51 to 1.65 m	Normal	Normal weight	Very low risk
From 31 to 45 kg	From 50 to 60 years	Female	From 1.51 to 1.65 m	High	Pre-obesity	Low risk
From 46 to 60 kg	From 50 to 60 years	Male	From 1.51 to 1.65 m	Hypertension level one	Class 1 obesity	Moderate
From 61 to 75 kg	From 50 to 60 years	Female	From 1.51 to 1.65 m	Hypertension level two	Class 2 obesity	High risk
From 31 to 45 kg	Over 60 years	Female	From 1.66 to 1.80 m	High	Pre-obesity	Low risk
From 46 to 60 kg	Over 60 years	Male	From 1.66 to 1.80 m	Hypertension level one	Class 1 obesity	Moderate
From 1.66 to 1.80 m	Over 60 years	Male	From 1.66 to 1.80 m	Hypertension level two	Class 2 obesity	High risk
Over 76 kg	Over 60 years	Female	From 1.66 to 1.80 m	Hypertension crisis	Class 3 obesity	Very high risk
From 15 to 30 kg	Over 60 years	Male	Over 1.80 m	Normal	Normal weight	Very low risk
From 31 to 45 kg	Over 60 years	Female	Over 1.80 m	High	Pre-obesity	Low risk
From 46 to 60 kg	Over 60 years	Male	Over 1.80 m	Hypertension level one	Class 1 obesity	Moderate
From 61 to 75 kg	Over 60 years	Male	Over 1.80 m	Hypertension level two	Class 2 obesity	High risk
From 31 to 45 kg	Under 20 years	Female	From 0.90 to 1.30 m	Hypertension level one	Class 1 obesity	Moderate
From 31 to 45 kg	Under 20 years	Male	From 1.31 to 1.50 m	Hypertension level one	Class 1 obesity	Moderate
From 31 to 45 kg	Under 20 years	Male	From 1.51 to 1.65 m	Hypertension level one	Class 1 obesity	Moderate
From 31 to 45 kg	From 20 to 35 years	Male	From 1.66 to 1.80 m	Hypertension level two	Class 2 obesity	High risk
From 31 to 45 kg	From 20 to 35 years	Female	Over 1.80 m	Hypertension level two	Class 2 obesity	High risk
From 31 to 45 kg	Under 20 years	Male	From 0.90 to 1.30 m	Hypertension crisis	Class 3 obesity	Very high risk
From 31 to 45 kg	From 20 to 35 years	Male	From 1.31 to 1.50 m	High	Pre-obesity	Low risk
From 46 to 60 kg	From 20 to 35 years	Female	From 1.51 to 1.65 m	Normal	Normal weight	Very low risk
From 46 to 60 kg	From 20 to 35 years	Female	From 1.51 to 1.65 m	Hypertension level two	Class 2 obesity	High risk
Over 76 kg	From 50 to 60 years	Male	Over 1.80 m	Normal	Normal weight	Very low risk
From 61 to 75 kg	From 36 to 49 years	Male	From 1.66 to 1.80 m	High	Class 1 obesity	Moderate
From 61 to 75 kg	From 20 to 35 years	Male	Over 1.80 m	Hypertension crisis	Class 3 obesity	Very high risk
Over 76 kg	From 50 to 60 years	Male	From 1.51 to 1.65 m	Hypertension level two	Pre-obesity	Moderate
From 31 to 45 kg	From 50 to 60 years	Male	From 1.66 to 1.80 m	Hypertension level one	Normal weight	Low risk
From 61 to 75 kg	From 20 to 35 years	Female	From 1.51 to 1.65 m	High	Class 1 obesity	Moderate
From 46 to 60 kg	From 36 to 49 years	Male	From 1.51 to 1.65 m	Hypertension level two	Pre-obesity	Moderate
From 61 to 75 kg	Over 60 years	Male	From 1.31 to 1.50 m	Hypertension level two	Class 3 obesity	Very high risk
Over 76 kg	From 36 to 49 years	Female	Over 1.80 m	Hypertension level one	Class 2 obesity	Very high risk
From 61 to 75 kg	From 50 to 60 years	Female	From 1.66 to 1.80 m	Hypertension level one	Class 1 obesity	Moderate

References

- Iso, H.; Cui, R.; Takamoto, I.; Kiyama, M.; Saito, I.; Okamura, T.; Miyamoto, Y.; Higashiyama, A.; Kiyohara, Y.; Ninomiya, T.; et al. Risk, Classification for Metabolic Syndrome and the Incidence of Cardiovascular Disease in Japan With Low Prevalence of Obesity: A Pooled Analysis of 10 Prospective Cohort Studies. *J. Am. Heart Assoc.* **2021**, *10*, e020760. [CrossRef]
- Poteat, T.C.; Rich, A.J.; Jiang, H.; Wirtz, A.L.; Radix, A.; Reisner, S.L.; Harris, A.B.; Cannon, C.M.; Lesko, C.R.; Malik, M.; et al. Cardiovascular Disease Risk Estimation for Transgender and Gender-Diverse Patients: Cross-Sectional Analysis of Baseline Data From the LITE Plus Cohort Study. *AJPM Focus* **2023**, *2*, 100096. [CrossRef]
- Landi, F.; Calvani, R.; Picca, A.; Tosato, M.; Martone, A.M.; Ortolani, E.; Sisto, A.; D’Angelo, E.; Serafini, E.; Desideri, G.; et al. Body Mass Index is Strongly Associated with Hypertension: Results from the Longevity Check-Up 7+ Study. *Nutrients* **2018**, *10*, 1976. [CrossRef]
- Oliveira, B.R.d.; Magalhães, E.I.d.S.; Bragança, M.L.B.M.; Coelho, C.C.N.d.S.; Lima, N.P.; Bettiol, H.; Barbieri, M.A.; Cardoso, V.C.; Santos, A.M.d.; Horta, B.L.; et al. Performance of Body Fat Percentage, Fat Mass Index and Body Mass Index for Detecting Cardiometabolic Outcomes in Brazilian Adults. *Nutrients* **2023**, *15*, 2974. [CrossRef]
- Lemieux, I.; Després, J.-P. Metabolic Syndrome: Past, Present and Future. *Nutrients* **2020**, *12*, 3501. [CrossRef]
- Cichosz, S.L.; Rasmussen, N.H.; Vestergaard, P.; Hejlesen, O. Is predicted body-composition and relative fat mass an alternative to body-mass index and waist circumference for disease risk estimation? *Diabetes Metab. Syndr. Clin. Res. Rev.* **2022**, *16*, 102590. [CrossRef] [PubMed]
- Ball, G.D.; Sharma, A.K.; Moore, S.A.; Metzger, D.L.; Klein, D.; Morrison, K.M. Measuring severe obesity in pediatrics using body mass index-derived metrics from the Centers for Disease Control and Prevention and World Health Organization: A secondary analysis of CANadian Pediatric Weight management Registry (CANPWR) data. *Eur. J. Pediatr.* **2023**. [CrossRef] [PubMed]
- Wang, Y.; Wang, H.; Zhou, J.; Wang, J.; Wu, H.; Wu, J. Interaction between body mass index and blood pressure on the risk of vascular stiffness: A community-based cross-sectional study and implications for nursing. *Int. J. Nurs. Sci.* **2023**. [CrossRef]
- Ismail, W.N.; P. P., F.R.; Ali, M.A.S. A Meta-Heuristic Multi-Objective Optimization Method for Alzheimer’s Disease Detection Based on Multi-Modal Data. *Mathematics* **2023**, *11*, 957. [CrossRef]
- Rojas-Valenzuela, I.; Valenzuela, O.; Delgado-Marquez, E.; Rojas, F. Multi-Class Classifier in Parkinson’s Disease Using an Evolutionary Multi-Objective Optimization Algorithm. *Appl. Sci.* **2022**, *12*, 3048. [CrossRef]

11. Long, S.; Zhang, D.; Li, S.; Li, S. Two-Stage Multi-Objective Stochastic Model on Patient Transfer and Relief Distribution in Lockdown Area of COVID-19. *Int. J. Environ. Res. Public Health* **2023**, *20*, 1765. [[CrossRef](#)]
12. Gheibi, M.; Eftekhari, M.; Akrami, M.; Emrani, N.; Hajiaghahi-Keshteli, M.; Fathollahi-Fard, A.M.; Yazdani, M. A Sustainable Decision Support System for Drinking Water Systems: Resiliency Improvement against Cyanide Contamination. *Infrastructures* **2022**, *7*, 88. [[CrossRef](#)]
13. Jan, T.; Azami, P.; Iranmanesh, S.; Ameri Sianaki, O.; Hajiebrahimi, S. Determining the Optimal Restricted Driving Zone Using Genetic Algorithm in a Smart City. *Sensors* **2020**, *20*, 2276. [[CrossRef](#)]
14. Gargouri, M.A.; Hamani, N.; Mrabti, N.; Kermad, L. Optimization of the Collaborative Hub Location Problem with Metaheuristics. *Mathematics* **2021**, *9*, 2759. [[CrossRef](#)]
15. Guo, L.; Xie, X.; Zeng, J.; An, N.; Wang, Z.; Gao, L.; Wang, Y.; Yang, J. Optimization Model of Water Resources Allocation in Coal Mine Area Based on Ecological Environment Priority. *Water* **2023**, *15*, 1205. [[CrossRef](#)]
16. Arumugham, V.; Ghanimi, H.M.A.; Pustokhin, D.A.; Pustokhina, I.V.; Ponnamp, V.S.; Alharbi, M.; Krishnamoorthy, P.; Sengan, S. An Artificial-Intelligence-Based Renewable Energy Prediction Program for Demand-Side Management in Smart Grids. *Sustainability* **2023**, *15*, 5453. [[CrossRef](#)]
17. Velluzzi, F.; Deledda, A.; Lombardo, M.; Fosci, M.; Crnjar, R.; Grossi, E.; Sollai, G. Application of Artificial Neural Networks (ANN) to Elucidate the Connections among Smell, Obesity with Related Metabolic Alterations, and Eating Habit in Patients with Weight Excess. *Metabolites* **2023**, *13*, 206. [[CrossRef](#)]
18. García-Sánchez, A.; Gómez-Hermosillo, L.; Casillas-Moreno, J.; Pacheco-Moisés, F.; Campos-Bayardo, T.I.; Román-Rojas, D.; Miranda-Díaz, A.G. Prevalence of Hypertension and Obesity: Profile of Mitochondrial Function and Markers of Inflammation and Oxidative Stress. *Antioxidants* **2023**, *12*, 165. [[CrossRef](#)]
19. Filist, S.; Al-kasasbeh, R.T.; Shatalova, O.; Aikeyeva, A.; Korenevskiy, N.; Shaqadan, A.; Trifonov, A.; Ilyash, M. Developing neural network model for predicting cardiac and cardiovascular health using bioelectrical signal processing. *Comput. Methods Biomech. Biomed. Eng.* **2022**, *25*, 908–921. [[CrossRef](#)] [[PubMed](#)]
20. Visco, V.; Izzo, C.; Mancusi, C.; Rispoli, A.; Tedeschi, M.; Virtuoso, N.; Giano, A.; Gioia, R.; Melfi, A.; Serio, B.; et al. Artificial Intelligence in Hypertension Management: An Ace up Your Sleeve. *J. Cardiovasc. Dev. Dis.* **2023**, *10*, 74. [[CrossRef](#)]
21. Lee, S.-J.; Lee, S.-H.; Choi, H.-I.; Lee, J.-Y.; Jeong, Y.-W.; Kang, D.-R.; Sung, K.-C. Deep Learning Improves Prediction of Cardiovascular Disease-Related Mortality and Admission in Patients with Hypertension: Analysis of the Korean National Health Information Database. *J. Clin. Med.* **2022**, *11*, 6677. [[CrossRef](#)] [[PubMed](#)]
22. Cocianu, C.-L.; Usatu, C.R.; Kofidis, K.; Muraru, S.; Văduva, A.G. Classical, Evolutionary, and Deep Learning Approaches of Automated Heart Disease Prediction: A Case Study. *Electronics* **2023**, *12*, 1663. [[CrossRef](#)]
23. Taylan, O.; Alkabaa, A.S.; Alqabbaa, H.S.; Pamukçu, E.; Leiva, V. Early Prediction in Classification of Cardiovascular Diseases with Machine Learning, Neuro-Fuzzy and Statistical Methods. *Biology* **2023**, *12*, 117. [[CrossRef](#)] [[PubMed](#)]
24. Chetoui, M.; Akhloufi, M.A.; Yousefi, B.; Bouattane, E.M. Explainable COVID-19 Detection on Chest X-rays Using an End-to-End Deep Convolutional Neural Network Architecture. *Big Data Cogn. Comput.* **2021**, *5*, 73. [[CrossRef](#)]
25. Luca, A.-C.; Curpan, A.-S.; Braha, E.E.; Țarcă, E.; Iordache, A.-C.; Luca, F.-A.; Adumitrachioaiei, H. Increasing Trends in Obesity-Related Cardiovascular Risk Factors in Romanian Children and Adolescents-Retrospective Study. *Healthcare* **2022**, *10*, 2452. [[CrossRef](#)] [[PubMed](#)]
26. Wang, Q.; Song, X.; Du, S.; Du, W.; Su, C.; Zhang, J.; Zhang, X.; Jia, X.; Ouyang, Y.; Li, L.; et al. Multiple Trajectories of Body Mass Index and Waist Circumference and Their Associations with Hypertension and Blood Pressure in Chinese Adults from 1991 to 2018: A Prospective Study. *Nutrients* **2023**, *15*, 751. [[CrossRef](#)]
27. Martins, M.; Mascarenhas, M.; Afonso, J.; Ribeiro, T.; Cardoso, P.; Mendes, F.; Cardoso, H.; Andrade, P.; Ferreira, J.; Macedo, G. Deep-Learning and Device-Assisted Enteroscopy: Automatic Panendoscopic Detection of Ulcers and Erosions. *Medicina* **2023**, *59*, 172. [[CrossRef](#)]
28. Cai, Y.; Hao, R.; Yu, S.; Wang, C.; Hu, G. Comparison of two multi-objective optimization methods for composite radiation shielding materials. *Appl. Radiat. Isot.* **2020**, *159*, 109061. [[CrossRef](#)]
29. Petchrompo, S.; Coit, D.W.; Brintrup, A.; Wannakrairot, A.; Parlikad, A.K. A review of Pareto pruning methods for multi-objective optimization. *Comput. Ind. Eng.* **2022**, *167*, 108022. [[CrossRef](#)]
30. Coello, C.; Van Veldhuizen, D.; Lamont, G. *Evolutionary Algorithms for Solving Multi-Objective Problems*, 2nd ed.; Springer: New York, NY, USA, 2007. [[CrossRef](#)]
31. Coello, C.A.; Lechuga, M.S. MOPSO: A proposal for multiple objective particle swarm optimization. *IEEE Congr. Evol. Comput.* **2002**, *2*, 1051–1056. [[CrossRef](#)]
32. Rachmawati, L.; Srinivasan, D. Multiobjective Evolutionary Algorithm With Controllable Focus on the Knees of the Pareto Front. *IEEE Trans. Evol. Comput.* **2009**, *13*, 810–824. [[CrossRef](#)]
33. Zitzler, E.; Thiele, L. An evolutionary algorithm for multiobjective optimization: The strength Pareto approach. In *Computer Engineering and Networks Laboratory (TIK)*; Technical Report 43; Swiss Federal Institute of Technology (ETH): Zurich, Switzerland, 1999.
34. Zitzler, E.; Thiele, L. Multiobjective evolutionary algorithms: A comparative case study and the strength Pareto approach. *IEEE Trans. Evol. Comput.* **1999**, *3*, 257–271. [[CrossRef](#)]

35. Knowles, J.; Corne, D. The Pareto archived evolution strategy: A new baseline algorithm for Pareto multiobjective optimization. In Proceedings of the 1999 Congress on Evolutionary Computation-CEC99, Washington, DC, USA, 6–9 July 1999; Volume 1, pp. 98–105. [[CrossRef](#)]
36. Corne, D.; Knowles, J.; Oates, M. The Pareto envelope-based selection algorithm for multiobjective optimization. In *Parallel Problem Solving from Nature-PPSN VI*; Springer: Berlin/Heidelberg, Germany, 2000; pp. 839–848. [[CrossRef](#)]
37. Deb, K.; Agrawal, S.; Pratap, A.; Meyarivan, T. A fast elitist non-dominated sorting genetic algorithm for multi-objective optimization: NSGA II. *IEEE Trans. Evol. Comput.* **2002**, *6*, 182–197. [[CrossRef](#)]
38. Zitzler, E.; Laumanns, M.; Thiele, L. SPEA 2: Improving the Strength Pareto Evolutionary algorithm. In *Computer Engineering and Networks Laboratory (TIK)*; Technical Report 103; Swiss Federal Institute of Technology (ETH): Zurich, Switzerland, 2001.
39. Dumitrescu, D.; Grosan, C.; Oltean, M. A new evolutionary adaptive representation paradigm. *Stud. Univ. Babeş Bolyai Ser. Inform.* **2001**, *46*, 19–28.
40. Meza, J.; Espitia, H.; Montenegro, C.; González, R. Statistical analysis of a multi-objective optimization algorithm based on a model of particles with vorticity behavior. *Soft Comput.* **2016**, *20*, 3521–3536. [[CrossRef](#)]
41. Meza, J.; Espitia, H.; Montenegro, C.; Giménez, E.; González, R. MOVPSO: Vortex Multi-Objective Particle Swarm Optimization. *Appl. Soft Comput.* **2017**, *52*, 1042–1057. [[CrossRef](#)]
42. Wen-Fung, L.; Yen, G. Dynamic swarms in PSO-based multiobjective optimization. In Proceedings of the 2007 IEEE Congress on Evolutionary Computation, Singapore, 25–28 September 2007. [[CrossRef](#)]
43. Zhi-Hui, Z.; Jingjing, L.; Jiannong, C.; Jun, Z. Multiple Populations for Multiple Objectives: A Coevolutionary Technique for Solving Multiobjective Optimization Problems. *IEEE Trans. Cybern.* **2013**, *43*, 445–463. [[CrossRef](#)]
44. Sun, Y.; Gao, Y.; Shi, X. Chaotic Multi-Objective Particle Swarm Optimization Algorithm Incorporating Clone Immunity. *Mathematics* **2019**, *7*, 146. [[CrossRef](#)]
45. Pellegrini, R.; Serani, A.; Liuzzi, G.; Rinaldi, F.; Lucidi, S.; Diez, M. Hybridization of Multi-Objective Deterministic Particle Swarm with Derivative-Free Local Searches. *Mathematics* **2020**, *8*, 546. [[CrossRef](#)]
46. You, Q.; Sun, J.; Pan, F.; Palade, V.; Ahmad, B. DMO-QPSO: A Multi-Objective Quantum-Behaved Particle Swarm Optimization Algorithm Based on Decomposition with Diversity Control. *Mathematics* **2021**, *9*, 1959. [[CrossRef](#)]
47. Bejarano, L.A.; Espitia, H.E.; Montenegro, C.E. Clustering Analysis for the Pareto Optimal Front in Multi-Objective Optimization. *Computation* **2022**, *10*, 37. [[CrossRef](#)]
48. Hussain, A.; Kim, H.-M. Evaluation of Multi-Objective Optimization Techniques for Resilience Enhancement of Electric Vehicles. *Electronics* **2021**, *10*, 3030. [[CrossRef](#)]
49. Qi, Y.; Zhang, Q.; Ma, X.; Quan, Y.; Miao, Q. Utopian point based decomposition for multi-objective optimization problems with complicated Pareto fronts. *Appl. Soft Comput.* **2017**, *61*, 844–859. [[CrossRef](#)]
50. Yan, J.; Li, C.; Wang, Z.; Deng, L.; Sun, D. Diversity Metrics in Multi-objective Optimization: Review and Perspectives. In Proceedings of the 2007 IEEE International Conference on Integration Technology, Shenzhen, China, 20–24 March 2007; pp. 553–557. [[CrossRef](#)]
51. Okabe, T.; Jin, Y.; Sendhoff, B. A Critical Survey of Performance Indices for Multi-Objective Optimisation. *Congr. Evol. Comput. CEC* **2003**, *2*, 878–885. [[CrossRef](#)]
52. Jiang, S.; Ong, Y.; Zhang, J.; Feng, L. Consistencies and Contradictions of Performance Metrics in Multiobjective Optimization. *IEEE Trans. Cybern.* **2014**, *44*, 2391–2404. [[CrossRef](#)]
53. Bhagavatula, S.S.; Sanjeevi, S.G.; Kumar, D.; Yadav, C.K. Multi-Objective Indicator Based Evolutionary Algorithm for Portfolio optimization. In Proceedings of the 2014 IEEE International Advance Computing Conference (IACC), Gurgaon, India, 21–22 February 2014; pp. 1206–1210. [[CrossRef](#)]
54. Cuate, O.; Schütze, O. Pareto Explorer for Finding the Knee for Many Objective Optimization Problems. *Mathematics* **2020**, *8*, 1651. [[CrossRef](#)]
55. Zhang, K.; Yen, G.G.; He, Z. Evolutionary Algorithm for Knee-Based Multiple Criteria Decision Making. *IEEE Trans. Cybern.* **2021**, *51*, 722–735. [[CrossRef](#)] [[PubMed](#)]
56. Szparaga, A.; Stachnik, M.; Czerwińska, E.; Kocira, S.; Dymkowska-Malesa, M.; Jakubowski, M. Multi-objective optimization based on the utopian point method applied to a case study of osmotic dehydration of plums and its storage. *J. Food Eng.* **2019**, *245*, 104–111. [[CrossRef](#)]
57. Mukhtaruddin, R.N.S.R.; Rahman, H.A.; Hassan, M.Y.; Jamian, J.J. Optimal hybrid renewable energy design in autonomous system using Iterative-Pareto-Fuzzy technique. *Int. J. Electr. Power Energy Syst.* **2015**, *64*, 242–249. [[CrossRef](#)]
58. Mateichyk, V.; Kostian, N.; Smieszek, M.; Mosciszewski, J.; Tarandushka, L. Evaluating Vehicle Energy Efficiency in Urban Transport Systems Based on Fuzzy Logic Models. *Energies* **2023**, *16*, 734. [[CrossRef](#)]
59. Zadeh, L.A. The concept of a linguistic variable and its application to approximate reasoning-I. *Inf. Sci.* **1975**, *8*, 199–249. [[CrossRef](#)]
60. Zadeh, L.A. Fuzzy logic and approximate reasoning. *Synthese* **1975**, *30*, 407–428. [[CrossRef](#)]
61. Tang, Y.; Jiacheng, Z. Linguistic modelling based on semantic similarity relation among linguistic labels. *Fuzzy Sets Syst.* **2006**, *157*, 1662–1673. [[CrossRef](#)]
62. Mazhar, T.; Nasir, Q.; Haq, I.; Kamal, M.M.; Ullah, I.; Kim, T.; Mohamed, H.G.; Alwadai, N. A Novel Expert System for the Diagnosis and Treatment of Heart Disease. *Electronics* **2022**, *11*, 3989. [[CrossRef](#)]

63. Wójcik, W.; Mezhiievska, I.; Pavlov, S.V.; Lewandowski, T.; Vlasenko, O.V.; Maslovskiy, V.; Volosovych, O.; Kobylanska, I.; Moskovchuk, O.; Ovcharuk, V.; et al. Medical Fuzzy-Expert System for Assessment of the Degree of Anatomical Lesion of Coronary Arteries. *Int. J. Environ. Res. Public Health* **2023**, *20*, 979. [[CrossRef](#)] [[PubMed](#)]
64. Lavie, C.J.; Arena, R.; Alpert, M.A.; Milani, R.V.; Ventura, H.O. Management of cardiovascular diseases in patients with obesity. *Nat. Rev. Cardiol.* **2017**, *15*, 45–56. [[CrossRef](#)]
65. Picca, A.; Mankowski, R.T.; Burman, J.L.; Donisi, L.; Kim, J.-S.; Marzetti, E.; Leeuwenburgh, C. Mitochondrial quality control mechanisms as molecular targets in cardiac ageing. *Nat. Rev. Cardiol.* **2018**, *15*, 543–554. [[CrossRef](#)] [[PubMed](#)]
66. O’Neil, A.; Scovelle, A.J.; Milner, A.J.; Kavanagh, A. Gender/Sex as a Social Determinant of Cardiovascular Risk. *Circulation* **2018**, *137*, 854–864. [[CrossRef](#)] [[PubMed](#)]
67. Khan, S.S.; Ning, H.; Wilkins, J.T.; Allen, N.; Carnethon, M.; Berry, J.D.; Lloyd-Jones, D.M. Association of Body Mass Index With Lifetime Risk of Cardiovascular Disease and Compression of Morbidity. *JAMA Cardiol.* **2018**, *3*, 280. [[CrossRef](#)]
68. Chrysant, S.G. Aggressive systolic blood pressure control in older subjects: benefits and risks. *Postgrad. Med.* **2018**, *130*, 159–165. <https://..> [[CrossRef](#)]
69. Chew, H.S.J.; Loong, S.S.E.; Lim, S.L.; Tam, W.S.W.; Chew, N.W.S.; Chin, Y.H.; Chao, A.M.; Dimitriadis, G.K.; Gao, Y.; So, B.Y.J.; et al. Socio-Demographic, Behavioral and Psychological Factors Associated with High BMI among Adults in a Southeast Asian Multi-Ethnic Society: A Structural Equation Model. *Nutrients* **2023**, *15*, 1826. [[CrossRef](#)] [[PubMed](#)]
70. Teo, K.K.; Rafiq, T. Cardiovascular Risk Factors and Prevention: A Perspective From Developing Countries. *Can. J. Cardiol.* **2021**, *37*, 733–743. [[CrossRef](#)] [[PubMed](#)]
71. Gabriel, R.; Brotons, C.; Tormo, J.; Segura, A.; Rigo, F.; Elosua, R.; Carbayo, J.A.; Gavrila, D.; Moral, I.; Tuomilehto, J.; et al. The ERICE-score: The New Native Cardiovascular Score for the Low-risk and Aged Mediterranean Population of Spain. *Rev. Esp. Cardiol.* **2015**, *68*, 205–215. [[CrossRef](#)]
72. Ministerio de Salud y Protección Social. Atención Médica del Año 2018 [Conjunto de datos] Minsalud 2018. Available online: <https://www.datos.gov.co/Salud-y-Proteccion-Social/Atencion-medica-del-a-o-2018/uerx-z994> (accessed on 8 September 2022).
73. MathWorks®. gamultiobj. Available online: <https://la.mathworks.com/help/gads/gamultiobj.html> (accessed on 10 November 2022).
74. Ishibuchi, H.; Sakane, Y.; Tsukamoto, N.; Nojima, Y. Evolutionary many-objective optimization by NSGA-II and MOEA/D with large populations. In Proceedings of the 2009 IEEE international conference on Systems, Man and Cybernetics, San Antonio, TX, USA, 11–14 October 2009; pp. 1758–1763. [[CrossRef](#)]
75. Rosenthal, S.; Borschbach, M. Impact of Population Size, Selection and Multi-Parent Recombination within a Customized NSGA-II and a Landscape Analysis for Biochemical Optimization. *Int. J. Adv. Life Sci.* **2014**, *6*, 310–324. Available online: https://www.thinkmind.org/articles/lifsci_v6_n34_2014_22.pdf (accessed on 10 November 2022).
76. Garbaruk, J.; Logofătu, D. Convergence Behaviour of Population Size and Mutation Rate for NSGA-II in the Context of the Traveling Thief Problem. *Lect. Notes Comput. Sci.* **2020**, *12496*, 164–175. [[CrossRef](#)]
77. Hort, M.; Sarro, F. The effect of offspring population size on NSGA-II: A preliminary study. In Proceedings of the Genetic and Evolutionary Computation Conference Companion, Lille, France, 10–14 July 2021; pp. 179–180. [[CrossRef](#)]
78. Zheng, W.; Liu, Y.; Doerr, B. A first mathematical runtime analysis of the non-dominated sorting genetic algorithm II (NSGA-II): (hot-off-the-press track at GECCO 2022). In Proceedings of the Genetic and Evolutionary Computation Conference Companion, Boston, MA, USA, 9–13 July 2022; pp. 53–54. [[CrossRef](#)]

Disclaimer/Publisher’s Note: The statements, opinions and data contained in all publications are solely those of the individual author(s) and contributor(s) and not of MDPI and/or the editor(s). MDPI and/or the editor(s) disclaim responsibility for any injury to people or property resulting from any ideas, methods, instructions or products referred to in the content.